JBC RESEARCH ARTICLE

FOXS1 is increased in liver fibrosis and regulates TGFβ responsiveness and proliferation pathways in human hepatic stellate cells

Received for publication, January 17, 2024 Published, Papers in Press, January 26, 2024,
https://doi.org/10.1016/j.jbc.2024.105691

Evelyn A. Bates[1], Zachary A. Kipp[1], Wang-Hsin Lee[1], Genesee J. Martinez[1], Lauren Weaver[2], Kathryn N. Becker[3], Sally N. Pauss[1], Justin F. Creeden[3], Garrett B. Anspach[4], Robert N. Helsley[4,5,6,7], Mei Xu[1], Maria E. C. Bruno[8], Marlene E. Starr[1,8], and Terry D. Hinds, Jr[1,6,7,*]

From the [1]Department of Pharmacology and Nutritional Sciences, University of Kentucky College of Medicine, Lexington, Kentucky, USA; [2]Department of Surgery, University of Minnesota, Minneapolis, Minnesota, USA; [3]Department of Neurosciences, University of Toledo College of Medicine and Life Sciences, Toledo, Ohio, USA; [4]Division of Endocrinology, Diabetes, and Metabolism, Department of Internal Medicine, and [5]Saha Cardiovascular Research Center, University of Kentucky College of Medicine, Lexington, Kentucky, USA; [6]Markey Cancer Center, University of Kentucky, Lexington, Kentucky, USA; [7]Barnstable Brown Diabetes Center, and [8]Division of Research, Department of Surgery, University of Kentucky College of Medicine, Lexington, Kentucky, USA

Reviewed by members of the JBC Editorial Board. Edited by Eric Fearon

Liver fibrosis commences with liver injury stimulating transforming growth factor beta (TGFβ) activation of hepatic stellate cells (HSCs), causing scarring and irreversible damage. TGFβ induces expression of the transcription factor Forkhead box S1 (FOXS1) in hepatocytes and may have a role in the pathogenesis of hepatocellular carcinoma (HCC). To date, no studies have determined how it affects HSCs. We analyzed human livers with cirrhosis, HCC, and a murine fibrosis model and found that FOXS1 expression is significantly higher in fibrotic livers but not in HCC. Next, we treated human LX2 HSC cells with TGFβ to activate fibrotic pathways, and FOXS1 mRNA was significantly increased. To study TGFβ-FOXS1 signaling, we developed human LX2 FOXS1 CRISPR KO and scrambled control HSCs. To determine differentially expressed gene transcripts controlled by TGFβ-FOXS1, we performed RNA-seq in the FOXS1 KO and control cells and over 400 gene responses were attenuated in the FOXS1 KO HSCs with TGFβ-activation. To validate the RNA-seq findings, we used our state-of-the-art PamGene PamStation kinase activity technology that measures hundreds of signaling pathways nonselectively in real time. Using our RNA-seq data, kinase activity data, and descriptive measurements, we found that FOXS1 controls pathways mediating TGFβ responsiveness, protein translation, and proliferation. Our study is the first to identify that FOXS1 may serve as a biomarker for liver fibrosis and HSC activation, which may help with early detection of hepatic fibrosis or treatment options for end-stage liver disease.

Hepatic dysfunction is becoming increasingly common due to the rise in obesity and its related comorbidities, such as insulin-resistant diabetes, nonalcoholic fatty liver disease (NAFLD), and other metabolic disarrangements dubbed "diseases of civilization" (1–3). The rates of NAFLD are rising and are expected to be over 30% of the world's adult population by 2030 (2, 4–6). NAFLD involves the benign accumulation of lipids in the liver (hepatic steatosis), a metabolic-related comorbidity (2). NAFLD can manifest as nonalcoholic steatohepatitis (NASH) (7), which is accompanied by inflammation and fibrosis (7–9); the latter causes liver scarring. NASH can further progress to cirrhosis, an irreversible end-stage fibrosis requiring a liver transplant. There are currently no Food and Drug Administration–approved drugs for treating NASH or cirrhosis that can reverse or improve liver scarring, making this aspect paramount to better understanding how to improve the disease.

Liver scarring commences through activating hepatic stellate cells (HSCs), which mainly, but not exclusively, arises from signaling by transforming growth factor beta (TGFβ) (8). When the liver is injured, hepatocytes release TGFβ to signal to the liver for repair. However, long-term chronic liver insults result in TGFβ-induced HSC activation and hepatic fibrosis (7). TGFβ activates the HSCs to proliferate and shed their extracellular matrixes, which are major culprits in the disease that causes scarring (7, 10). Recent studies have demonstrated that the transcription factor Forkhead box S1 (FOXS1) (*FKHL18* gene) is a TGFβ-induced responder in epithelial-mesenchymal transition (EMT) of hepatocytes in hepatocellular carcinoma (HCC) (11). However, its role in mediating liver fibrosis in TGFβ-induced HSC activation has not been revealed.

Here, we hypothesized that TGFβ-induced FOXS1 may have a role in liver fibrosis. We wanted to determine the signaling pathways during these events and whether FOXS1 is involved in TGFβ activation of HSCs. We measured FOXS1 levels in human cirrhotic livers, a mouse model of hepatic fibrosis, and in TGFβ-induced human HSC activation. To determine FOXS1's signaling functions, we developed FOXS1 CRISPR

* For correspondence: Terry D. Hinds, Terry.Hinds@uky.edu.

KO cells in human HSCs. Using our state-of-the-art PamGene PamStation technology that measures kinase activity in real time of hundreds of signaling events in a sample (7, 12, 13) and complementary RNA-seq analysis, we found that FOXS1 controls TGFβ-induced pathways for cell–cell adhesion, extracellular binding, and protein translation. These studies are the first to reveal the importance of the FOXS1 transcription factor in TGFβ-induced liver injury and activation of HSCs that lead to liver fibrosis and scarring.

Results

FOXS1 levels in cirrhotic human livers, fibrotic mouse livers, and cell models of liver fibrosis

To determine the level of FOXS1 in liver disease, we first used human cirrhotic and healthy livers and a murine model of fibrosis. In Figure 1, *A* and *B*, the Sirius red and trichrome blue staining show the level of fibrosis in healthy and cirrhotic human livers. A clinical pathologist scored the livers, and all human cirrhotic livers exhibited stage 4 fibrosis (described in (7)). The CCL_4 injury–induced mouse model had fibrotic livers at stage 3 (7), and healthy controls for humans and mice were at stage 0 (7). In the mouse fibrotic model, fibrosis was only observed at the 5-week CCL_4 treatment and not at 72 h (Fig. 1*B*). To determine if the expression levels of FOXS1 correlate with fibrotic events in human or mouse livers, we performed real-time PCR on these livers. There was a significant increase in *FHKL18* mRNA (FOXS1 gene) expression levels in cirrhotic samples and *Fhkl18* mRNA in the CCL_4 injury–induced mouse model of liver fibrosis (Fig. 1, *A* and *B*). In the fibrotic mouse model, there were no significant differences in *Fhkl18* or *Acta2* mRNA levels at the acute time treatment of 72 h; however, both were significantly increased with the 5-week CCL_4 treatment that had fibrosis (Fig. 1*B*). Activation of HSCs entails increases in smooth muscle actin (alpha-SMA), which also serves as a liver fibrosis biomarker (14). The gene that encodes alpha-SMA is *ACTA2*, which was significantly increased with both fibrotic groups (Fig. 1, *A* and *B*). Since FOXS1 had been reported to possibly be involved in HCC, we measured its mRNA expression in nine paired human HCC tumor tissue and adjacent nontumor tissue. No differences were observed for *FKHL18*, *ACTA2*, or *TGFB1* between HCC tumor tissue compared to adjacent nontumor tissue (Fig. 1*C*). This suggested that the major role of FOXS1 in the liver is likely in the HSCs and not hepatocytes. Therefore, we focused our work on the human LX2 HSC cell line.

To determine whether FOXS1 is increased in HSCs, we used the human LX2 HSC cell line treated with or without TGFβ in different serum conditions. The serum conditions were to mimic the "fed" or "fasted" states by using the normal serum for fed or dialyzed serum, with molecules less than 10 kDA removed, for fasting. The purpose of the fed and fasted serum conditions is to determine if FOXS1 responds to metabolic cues, which occurs in many liver-mediated signaling pathways (15, 16), such as with PPARα, which is highly expressed in the fasted state but not in the fed (17). The *FHKL18* mRNA was significantly (p = 0.0092 for fed and p = 0.0040 for fasted) increased with TGFβ treatment in both conditions, and no significant (p = 0.9084) differences between the fed and fasted TGFβ-treated groups were observed (Fig. 1*D*). These indicate that likely FOXS1 expression does not respond to metabolic stimuli. As expected, *ACTA2* was significantly higher in both TGFβ-treated groups. However, the fasted serum condition had significantly less *ACTA2* expression than the fed serum condition. These data indicate that FOXS1 may be involved in HSC activation and liver fibrosis.

CRISPR FOXS1 knockout in human HSCs and the impact on proliferation and migration

To create the FOXS1 KO and control human LX2 cell lines, we utilized CRISPR technology to remove part of the single exon that the FOXS1 gene contains (Fig. 2*A*). The *FKHL18* gene (FOXS1 protein) only has one exon and no introns, and the removal of nucleotides 145 to 316 causes the production of a nonfunctional protein. We validated the deletion of the 145 to 316 nucleotide region of the *FKHL18* gene using primers designed in the cut site with conventional PCR using genomic DNA (Fig. 2*A*). To determine the level of the FOXS1 in the KO and control cells, we treated them with 5 ng/ml TGFβ or vehicle for 24 h. We found a −92.4% reduction in *FHKL18* mRNA in the TGFβ treated FOXS1 KO LX2 cells compared to the scrambled control with the same treatments (Fig. 2*B*). To validate the FOXS1 KO at the protein level, we treated KO and scrambled control cells with 5 ng/ml TGFβ for 24 h. Similar to our mRNA results, we found that the FOXS1 protein is significantly increased with TGFβ treatment in scrambled control cells and that the FOXS1 protein levels were undetectable in KO cells (Fig. 2, *C* and *D*).

Determination of FOXS1-dependent gene networks

To determine the overall transcriptional effect of the TGFβ-FOXS1 signaling, we performed RNA-seq of the FOXS1 KO and scrambled control LX2 HSCs treated with 5 ng/uL TGFβ or vehicle for 24 h. We first analyzed differentially expressed genes (DEGs) and the overall expression of DEGs, which we visualized using a heatmap (Fig. 3*A*). The heatmap showed that the FOXS1 KO HSCs treated with TGFβ had reduced patterns of gene expression when compared to scrambled control HSCs, suggesting a subset of FOXS1 genes are mediated by TGFβ activation. Next, to examine DEGs controlled by TGFβ-FOXS1, we performed volcano plot analysis of the FOXS1 KO and scrambled control LX2 HSCs (TGFβ-vehicle) for each group (Fig. 3*B*). The significantly changed DEGs were identified, and a line was drawn to show genes statistically modified with TGFβ treatments in each group. The scrambled control HSCs had 2377 DEGs, and the FOXS1 KO HSCs had 1961 DEGs, indicating that 416 shared genes were lost in the FOXS1 KO HSCs. To show genes regulated by FOXS1, we used the gene lists with a cutoff of p adjusted < 0.05, and TGFβ treatments were subtracted from the vehicle (TGFβ-vehicle) for each condition to compare TGFβ-FOXS1–dependent actions. We displayed the data using a Venn diagram (Fig. 3*C*). There were 1403 shared genes among the scramble and

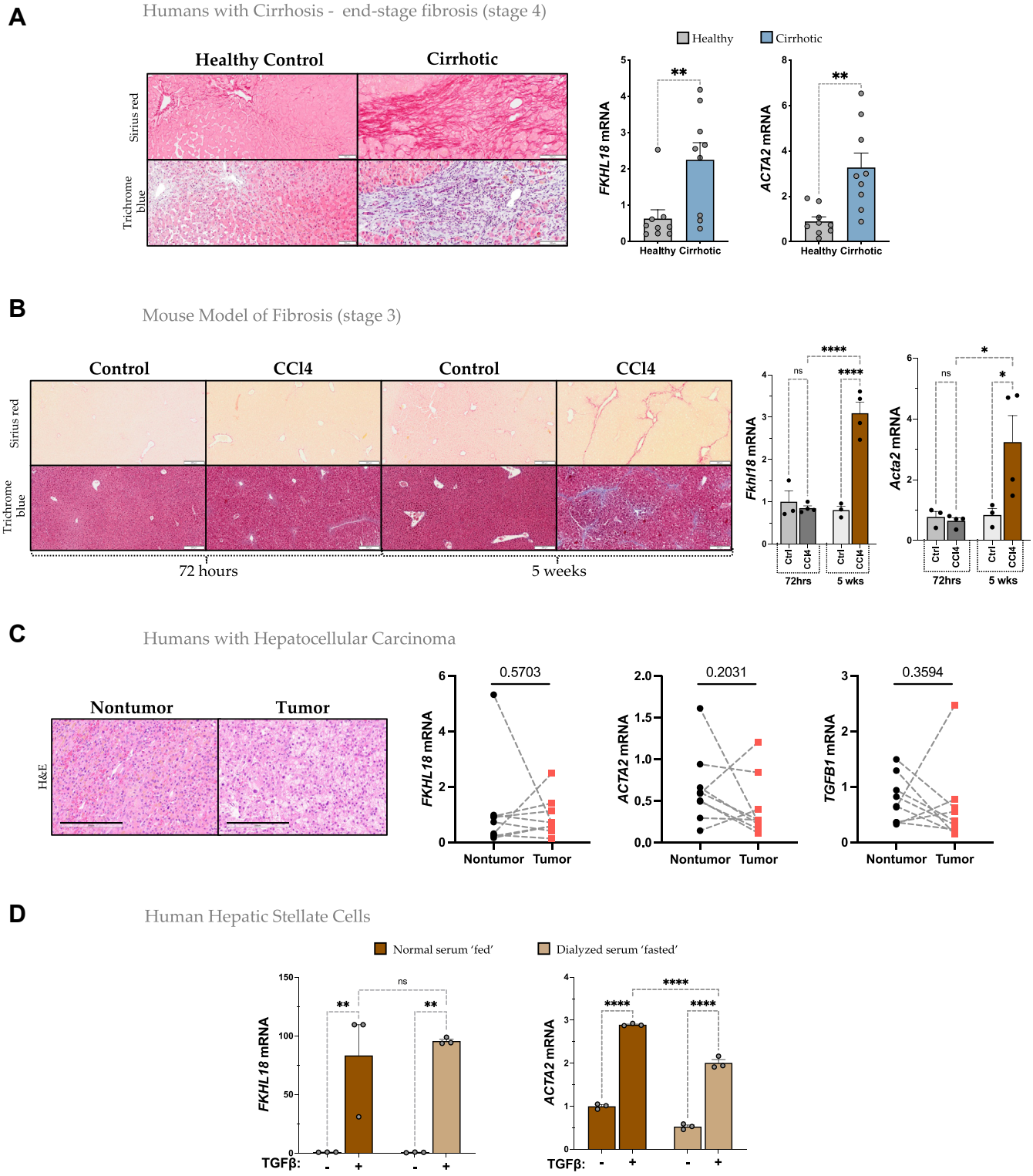

Figure 1. FOXS1 levels in human and murine fibrotic livers and activated hepatic stellate cells. *A*, human or (*B*) mouse livers were stained with *Sirius red* or *trichome blue* to indicate areas of liver fibrosis and real-time measurements of mRNA expression for *FKHL18* and *ACTA2* (*Fhkl18* and *Acta2* in mice). The scale bar represents 100 μm (*A*) and 200 μm (*B*); *$p < 0.05$; **$p < 0.01$; and ****$p < 0.0001$ *versus* control; (n = 9 for human cirrhotic livers and n = 3–4 for mouse livers). *C*, H&E staining of livers from patients with hepatocellular carcinoma (HCC) and measure of *FKHL18*, *ACTA2*, and *TGFB1* by real-time PCR of HCC cancerous regions and noncancerous regions from the same patient (n = 9). The scale bar represents 200 μm. *D*, the human LX2 HSC cell line was treated with TGFβ or vehicle for 24 h to activate the fibrotic pathways in both "fed" and "fasted" serum conditions. RNA was extracted for real-time PCR quantification of *FKHL18* and *ACTA2*. **$p < 0.01$ and ****$p < 0.0001$ (n = 3). FOXS1, Forkhead box S1; HSC, hepatic stellate cell; TGFβ, transforming growth factor beta.

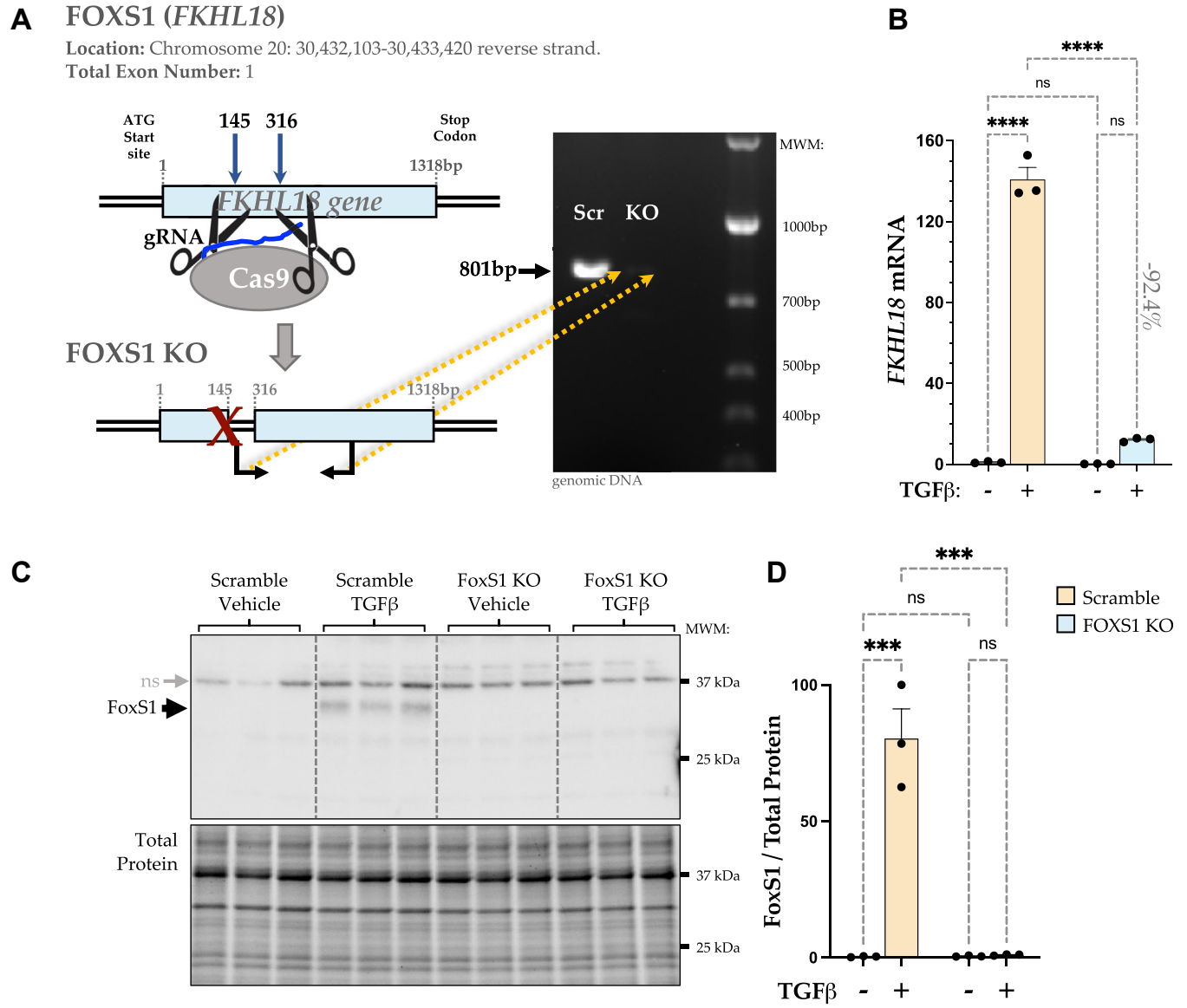

Figure 2. CRISPR knockout of FOXS1 in human hepatic stellate cells and the effect on TGFβ-induced proliferation and migration. *A*, generation of the CRISPR FOXS1 KO and scrambled control in human HSC LX2 cells. Using the CRISPR guide RNA system, the *FHKL18* gene was cut at sites 200 and 391 in exon 1, which was validated by conventional PCR using genomic DNA. *B*, the FOXS1 KO and scrambled control cells were treated with TGFβ or vehicle for 24 h, and the level of *FHKL18* mRNA was measured by real-time PCR. ****$p < 0.0001$; (n = 3). *C* and *D*, FOXS1 protein levels were quantified by immunoblotting in FOXS1 KO and scrambled control cells treated with TGFβ or vehicle for 24 h and normalized to total protein. FOXS1, Forkhead box S1; TGFβ, transforming growth factor beta.

FOXS1, 964 specific to scramble, and 548 unique to FOXS1 KO HSCs. Using the FOXS1-dependent DEGs, we performed Gene Ontology (GO) pathway analysis that was separated by biological, cellular, and molecular functions (Fig. 3*D*). We scored the pathways using a novel amalgamated enrichment score, which incorporated the number of genes associated with a pathway and the significance of the perturbation of the pathway. Included among the top GO biological functions controlled by FOXS1 are pathways such as cytoplasmic translation, positive regulation of protein localization to chromosome and Cajal body, peptide biosynthetic process, ribonucleoprotein complex biogenesis, regulation of Anoikis and cell migration, and several processes including translation, wound healing, and cell migration. In the GO cellular function, we identified several pathways involved in hepatic fibrosis, such as focal adhesion, cell-substrate junction, collagen-containing extracellular matrix, and many other pathways related to fibrosis, such as cell–cell junction, adherens junction, and cell–cell contact zone. The top pathways in the GO molecular functions were cadherin binding, platelet-derived growth factor binding, cyclin-dependent protein serine-threonine kinase (STK) inhibitor activity, protein binding involved in heterotypic cell–cell adhesion, neurotrophin binding, and processes involved in fibrosis, including peptidyl-proline 4-dioxygenase activity, procollagen-proline dioxygenase activity, and transforming factor beta receptor binding.

To confirm the results above, we validated some of the genes by real-time PCR that were identified in the analysis

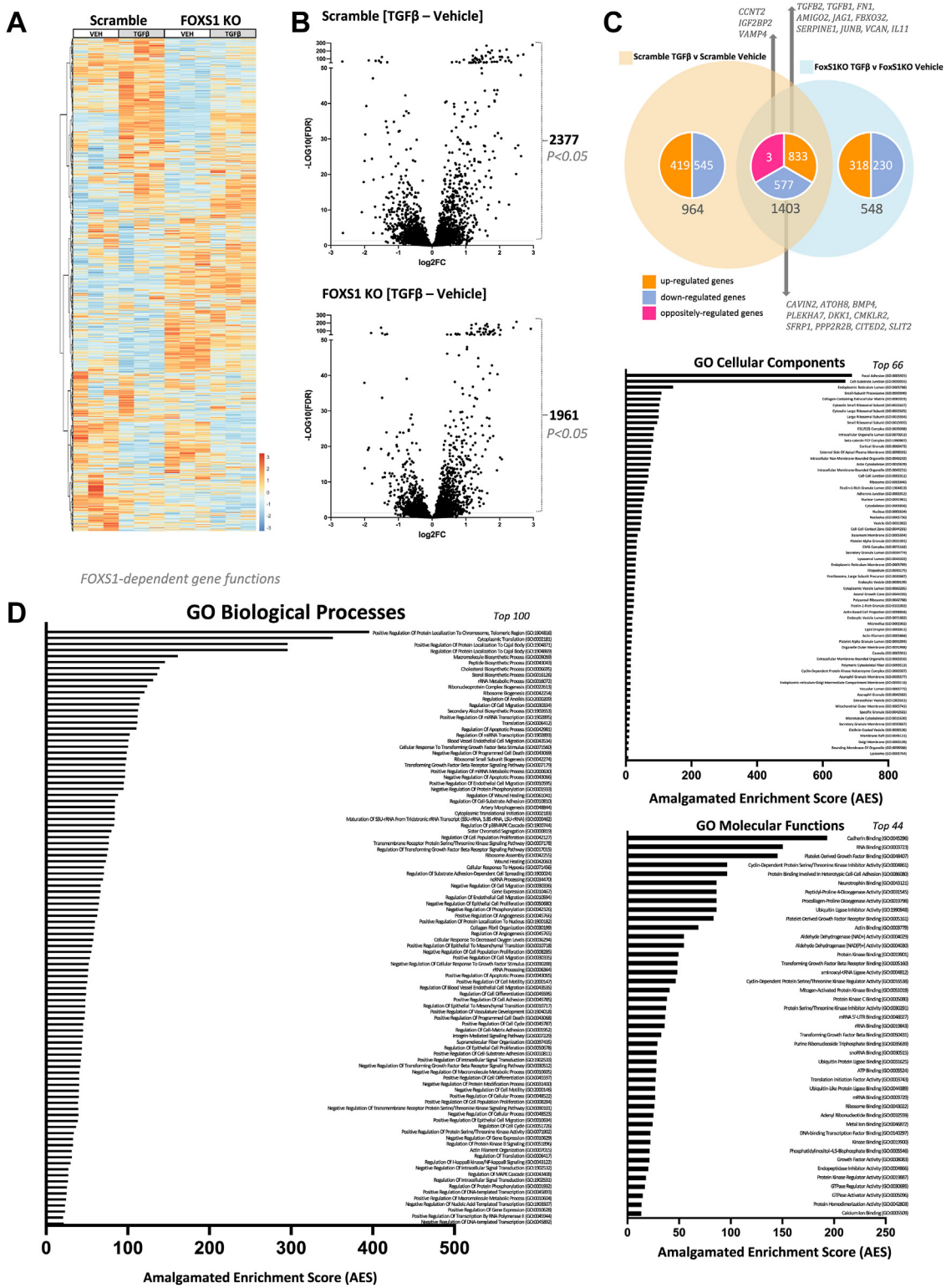

Figure 3. TGFβ-induced pathways in human FOXS1 KO and scrambled control hepatic stellate cells. The FOXS1 KO and scrambled control cells were treated with 5 ng/μl TGFβ or vehicle for 24 h, and RNA was extracted for RNA-seq. *A*, heatmap analysis of RNA-seq data. *B*, *volcano plots* of differentially expressed genes (DEGs) in LX2 scrambled control (TGFβ, vehicle) or FOXS1 KO cells (TGFβ, vehicle). The values on the right of the graphs are statistically significant changed genes. *C*, *venn diagram* of shared DEGs. To calculate the FOXS1-dependent genes, the DEGs were subtracted from the scrambled and FOXS1 KO (416 DEGs). *D*, the FOXS1-dependent genes were used for Gene Ontology (GO) pathway analysis, separated by biological, cellular, and molecular functions. Amalgamated enrichment score (AES) combines the GO combined score and significance value associated with each pathway. FOXS1, Forkhead box S1; TGFβ, transforming growth factor beta.

from Figure 3. We show groups of genes that were higher in the FOXS1 KO cells than the scrambled control (Fig. 4*A*), lower in KO (Fig. 4*B*), genes not changed between the control and KO groups (Fig. 4*C*), and genes known to be involved in fibrosis (Fig. 4*D*). We found that the loss of FOXS1 significantly impacted TGFβ-induced genes, which likely changes pathways within the HSCs. Therefore, to validate our pathway analysis from our RNA-seq data, we used our advanced PamGene kinome technology to measure the real-time kinase activity of hundreds of signaling pathways.

Determination of FOXS1-dependent kinase pathways

Our RNA-seq data largely addressed the transcriptional landscape resulting from the TGFβ–FOXS1 axis. However, to delve further into the actual pathways that the TGFβ–FOXS1 axis mediates, we utilized our PamGene PamStation advanced kinome technology. We wanted to validate the RNA-seq pathway analysis and identify possible therapeutic targets for the TGFβ-FOXS1 role in liver fibrosis. We have previously used the PamGene technology to identify kinases driving fibrotic pathways in humans with cirrhosis and three rodent models with liver fibrosis, two of which were NAFLD-NASH models with emerging fibrosis (7). To determine kinase pathways regulated by TGFβ-FOXS1, we quantified the kinase activity at 144 serine/threonine peptide substrates and 196 protein-tyrosine kinase (PTK) peptide substrates from the FOXS1 KO and scrambled LX2 HSCs treated with 5 ng/ml TGFβ or vehicle for 1 h. Our serine/threonine analysis revealed that the FOXS1 KO and Scrambled HSCs robustly responded to the TGFβ treatment and that some STKs were hyperactive with the loss of FOXS1, as shown by heatmap analysis of phosphorylated substrates (Fig. 5*A*). A waterfall plot of the substrates indicates that some peptide substrates were hyperphosphorylated and others were hypophosphorylated (Fig. 5*B*). To determine the kinases that phosphorylated the substrates, we performed an upstream analysis using normalized kinase statistics of the substrates (Fig. 5*C*). When plotted by log fold change of phosphorylated substrates, the most hyperactive were alpha kinase 1, intestinal cell kinase (ICK), extracellular-signaling regulated kinase (ERK) kinases, and several cyclin-dependent kinases (Fig. 5*D*). Next, we used random sampling significance analysis to identify the relative confidence of each selected kinase, shown as peacock plots. We used our peacock and MEOW plot analyses to show individual responses for the 12 most changed kinases in the waterfall plot in Figure 5*C*. The peacock plots show higher confidence for ICK, ERK1, ERK2, and CDKL2 kinases (Fig. 5*E*, top figures), which is reinforced when the delta confidence and log2FC are combined in the MEOW plots (Fig. 5*E*, bottom figures). Together, these indicate that ICK (also referred to as ciliogenesis-associated kinase 1) and alpha kinase 1 had 89.3% and 35.4% increased kinase activity, respectively (indicated by the blue line). Interestingly, ICK is thought to be critical in epithelial cell proliferation and differentiation and controls protein translation (18, 19). The increased activity measured in the FOXS1 KO from the STK PamChip data aligns with the findings from the RNA-seq data that the loss of FOXS1 activates pathways for translation.

The heatmap results for the PTK substrates showed responsiveness to TGFβ and vehicle treatments in the FOXS1 KO and scrambled HSCs (Fig. 6*A*). Further analyses of the PTK kinases comparing the FOXS1 KO TGFβ and Scrambled TGFβ treatments showed minimal differences for the tyrosine kinases, as shown in Figure 6, *B–E*. Most kinases generally showed average confidence intervals, with CSK and FLT4 showing the most significance in altered activity (Fig. 6*E*). We combined the relative confidence interval with the log fold change of substrates in the MEOW plots (Fig. 6*E*, bottom row), and these comprehensive plots further indicated that most tyrosine kinases were unchanged. However, Lmr1 PTK was increased in the FOXS1 KO compared to the scrambled control HSCs. Lmr1 has been demonstrated to be involved in regulating cell migration (20). The FOXS1 KO HSCs had slightly higher migration rates but did not change significantly, as shown in Figure 2. Overall, there were fewer effects from the loss of FOXS1 on tyrosine kinase pathways and more impact on serine–threonine pathways.

To visually represent the kinase activity demonstrating the phosphorylation level of the 340 kinase substrates, we used an upstream analysis performed with the data deconvoluted into a kinase tree for humans (Fig. 7). The phyla tree shows that many kinase pathways were changed. The most changed overall was ICK (indicated by the blue arrow). The size of the circle represents its Z score changed from scrambled control treated with the same treatments, with the color indicating the directionality of change (hyperactivity in ICK). To validate the ICK findings from the PamGene data, we performed immunoblotting of the FOXS1 KO and scrambled HSCs. We found that TGFβ treatments for 1 h significantly increased expression in the FOXS1 KO but not in the Scrambled HSCs with the same treatment (Fig. 8*A*). We also verified the findings from two kinase pathways that were not found to be significantly changed with the PamGene technology, which were ERK and JNK signaling pathways. We show in Figure 8*B* that phosphorylation of ERK and JNK was not changed with 1-h TGFβ treatments. Together, these support the findings from the PamGene kinase activity data.

Next, we determined if protein translation, proliferation, or migration pathways are affected by the loss of FOXS1, as the two omics analyses recommended. We found that protein translation using the puromycin incorporation assays showed that FOXS1 KO HSCs had significantly higher protein translation rates at 1 h but not at 24 h or with TGFβ treatments (Fig. 8*C*). To determine the effects of TGFβ treatments on HSC proliferation, we performed a cell growth assay with TGFβ treatment over 96 h. The FOXS1 KO cells had no significant (p = 0.1359) differences in growth by comparison of the area under the curve over the 96-h period compared to scrambled control LX2 cells (Fig. 8*D*). However, comparing the scramble and FOXS1 KO for specific time points at 72 and 96 h was statistically significant (p = 0.0191 at 72 h and p = 0.0054 at 96 h). Since FOXS1 KO cells were shown to be

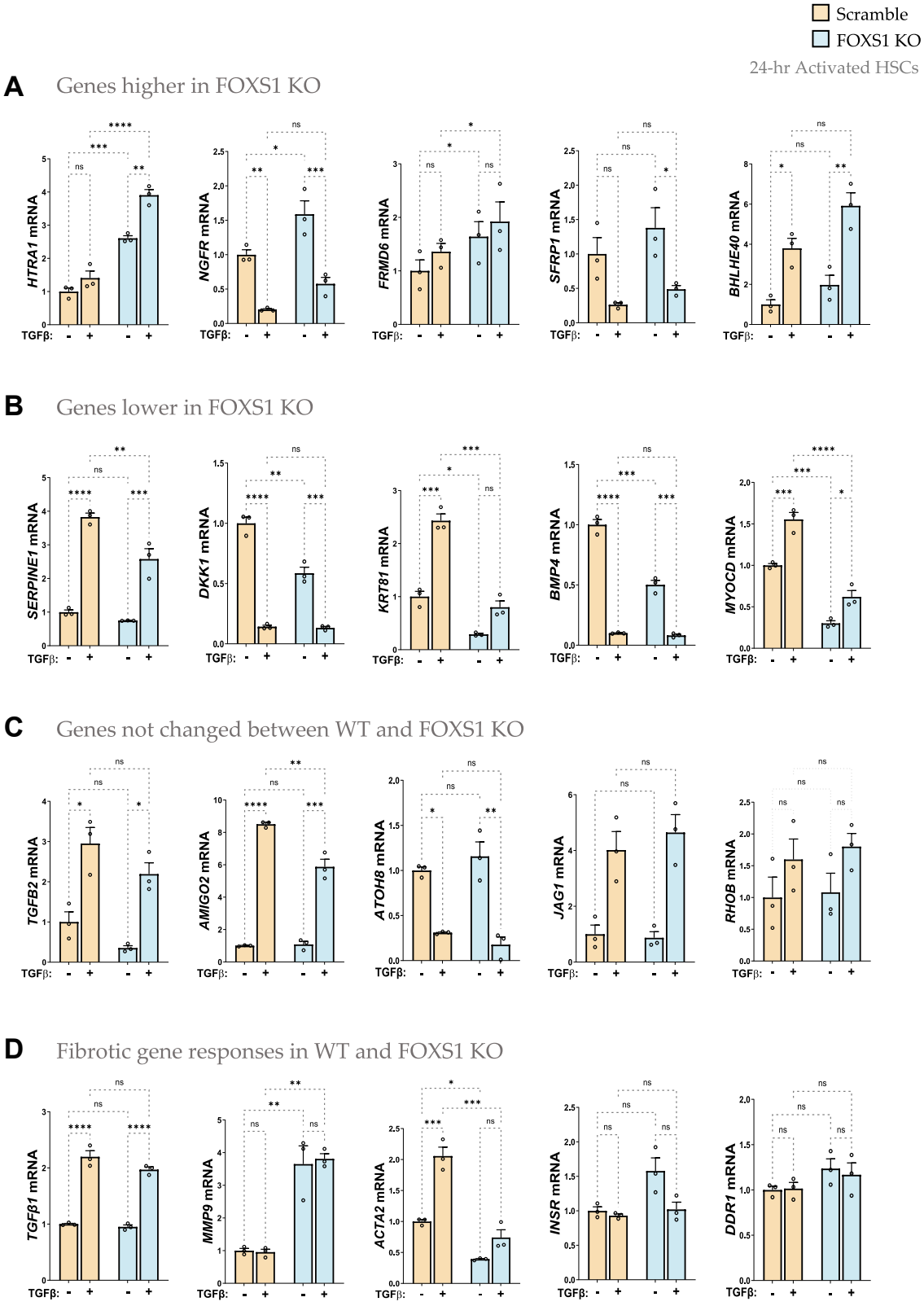

Figure 4. Measurements of DEGs changed between FOXS1 KO and scrambled LX2 cells treated with TGFβ. FOXS1 KO and scrambled HSCs were treated with TGFβ or vehicle for 24 h, and RNA was extracted for real-time PCR measurements of DEGs. *A*, DEGs higher in KO (*B*) DEGs lower in KO, (*C*) genes not changed between the control and KO groups, and (*D*) genes known to be involved in fibrosis. *$p < 0.05$; **$p < 0.01$; ***$p < 0.001$; and ****$p < 0.0001$; (n = 3). DEG, differentially expressed gene; FOXS1, Forkhead box S1; TGFβ, transforming growth factor beta.

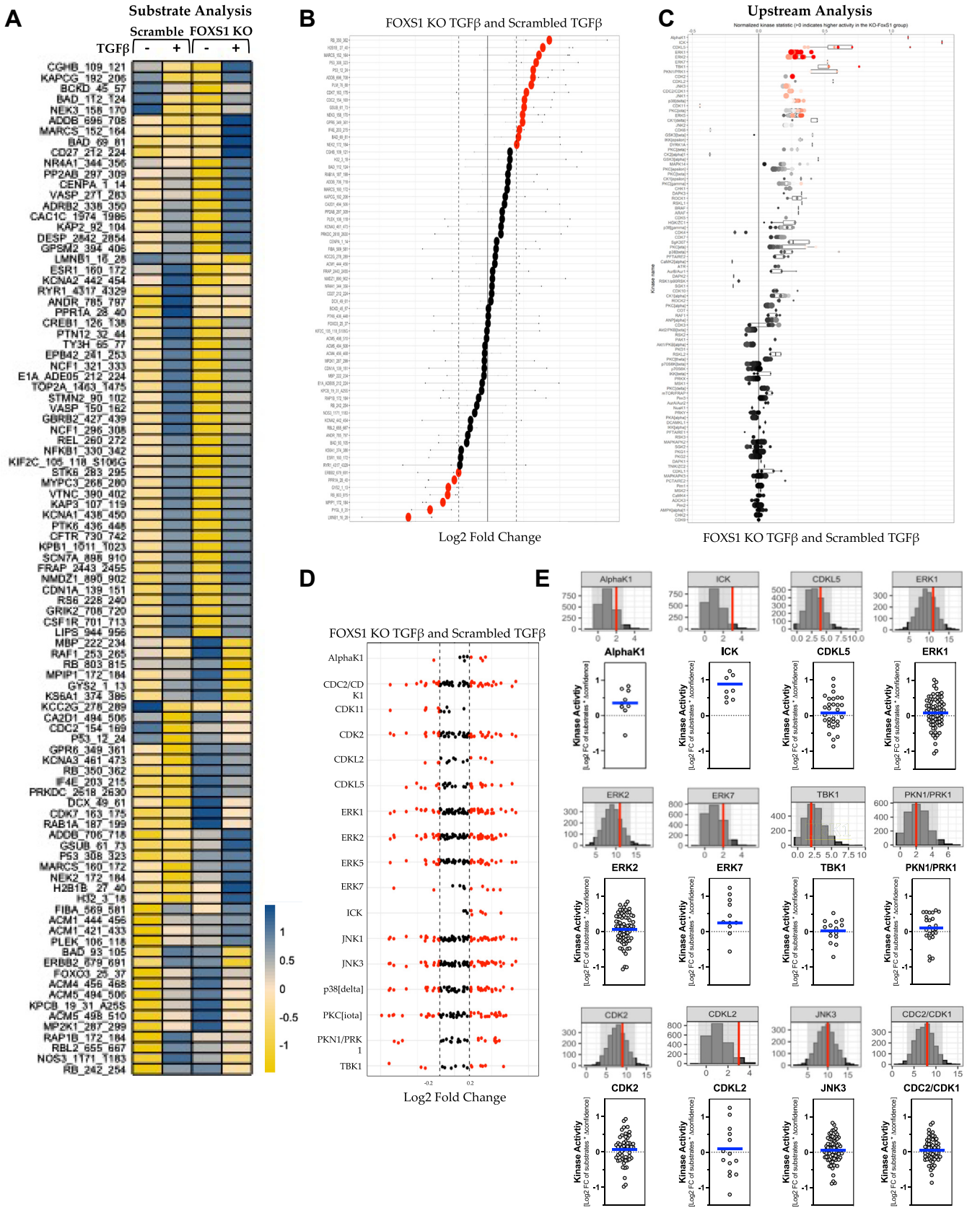

Figure 5. Serine-threonine kinase pathway activity. Heatmap analysis of differentially active kinases shows a pattern of kinase activity related to FOXS1 expression (*A*). Differentially phosphorylated substrates are relatively evenly split between hyperphosphorylation and hypophosphorylation (*B*). When individual kinases are plotted by mean kinase statistic, we identify a cluster of overactive kinases in the FOXS1 TGFβ treatment group (*C*). Individual kinases plotted by log fold change and individual substrates show a similar trend (*D*). A significance measure using 2000 random sampling iterations shows relatively high confidence in most top-hit kinases (*E*, *top figure*). When combined with the log fold change, the significance measures are more confident in each kinase, as displayed by MEOW plots (*E*, *bottom figure*). FOXS1, Forkhead box S1; TGFβ, transforming growth factor beta.

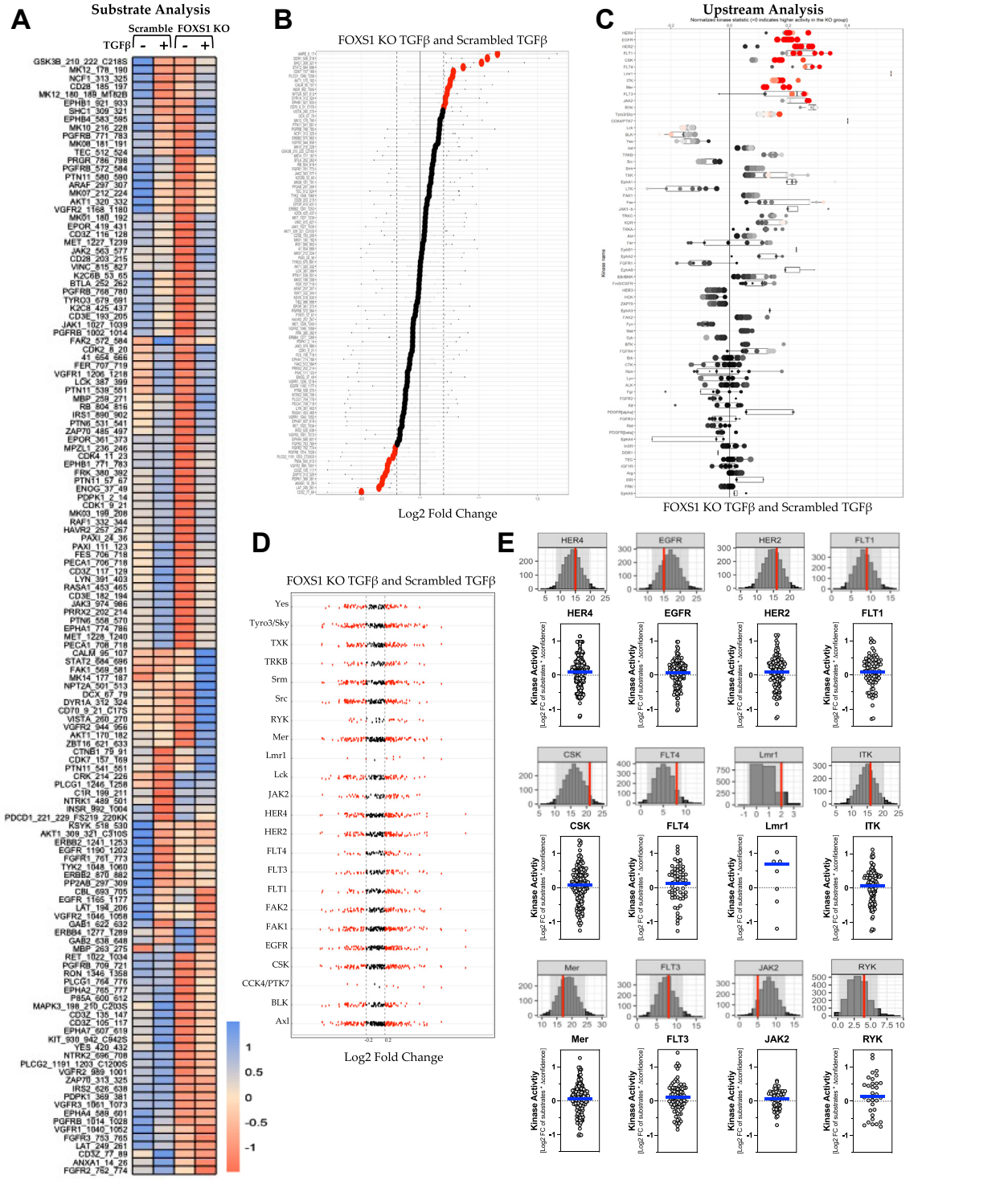

Figure 6. Protein-tyrosine kinase activity. Heatmap analysis of differentially active kinases shows a pattern of kinase activity related to FOXS1 expression (*A*). Differentially phosphorylated substrates are relatively evenly split between hyperphosphorylation and hypophosphorylation (*B*). When individual kinases are plotted by mean kinase statistic, we identify a cluster of overactive kinases in the FOXS1 TGFβ treatment group compared to the scrambled TGFβ group (*C*). Individual kinases plotted by log fold change and individual substrates show a similar trend (*D*). A significance measure using 2000 random sampling iterations shows relatively average confidence in most top-hit kinases (*E*, *top figure*). When combined with the log fold change, the significance measures are more confident in each kinase, as displayed by MEOW plots (*E*, *bottom figure*). The *blue line* indicates average activity across all measured substrates. FOXS1, Forkhead box S1; TGFβ, transforming growth factor beta.

important in the regulation of EMT (11), we conducted a cell migration assay using the transwell culturing system for the FOXS1 KO and scrambled LX2 HSCs treated with 5 ng/ml TGFβ or vehicle for 24 h. The TGFβ treatments in the scrambled LX2 HSCs reduced the cell count in the transwell at 24 h (Fig. 8*E*), which others have also observed, as shown in (21). However, the FOXS1 KO LX2 cells had no statistically significant differences (p = 0.0538) in migration with the TGFβ

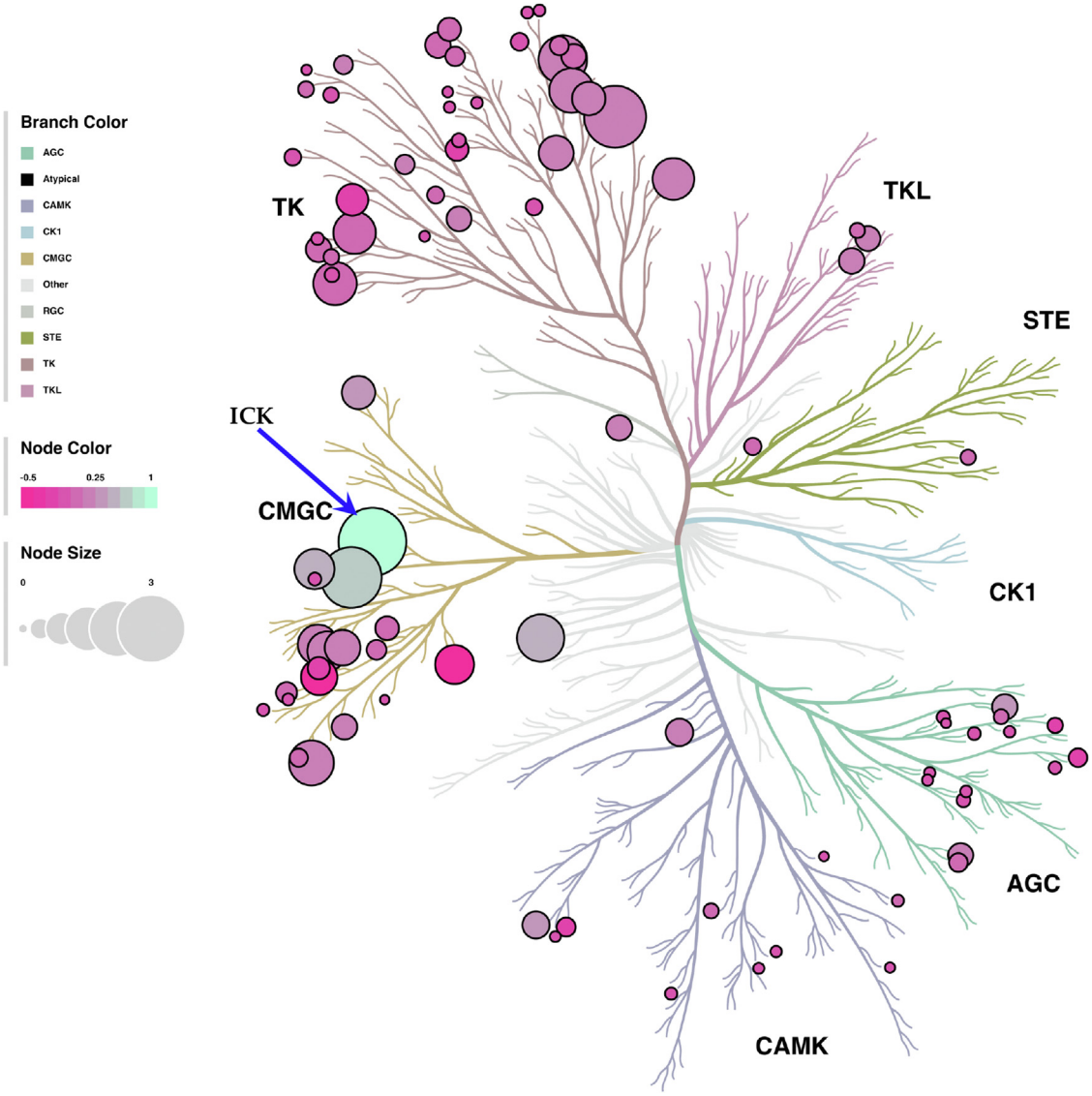

Figure 7. Paralogous phylogenic relationships between differentially altered kinases. The FOXS1 KO and scrambled HSCs with TGFβ treatments were compared using the STK and PTK data for analyses. Node color and size are the mean final kinase score corresponding to the *bubble plot* on the paralogous phylogenetic trees. FOXS1, Forkhead box S1; PTK, protein-tyrosine kinase; STK, serine-threonine kinase; TGFβ, transforming growth factor beta.

treatments. The cell count was lower in the vehicle-treated FOXS1 than in the scrambled control but not significantly different (p = 0.0625). These data indicate that FOXS1 in human HSCs may regulate cell proliferation and migration with TGFβ activation of fibrotic pathways.

Overall, these data indicate that FOXS1 has a role in liver fibrosis *via* HSCs to regulate TGFβ responsiveness, proliferation, protein translation, and possibly other pathways not directly measured here, such as cell–cell adhesion and other signaling functions described above.

Discussion

This is the first study to show the involvement of FOXS1 in TGFβ-induced HSC activation. While it is known that TGFβ activates HSCs to shed their extracellular matrices during activation of liver fibrosis, the intracellular signaling mechanisms of this disease are not fully understood. In our study, we found that FOXS1 cooperates with TGFβ activation of HSCs through the transcriptional control of genes that regulate cell–cell adhesion, junction, and contact zone, and pathways related to fibrosis, such as collagen-containing extracellular matrix, wound healing, and cell migration. Our study is the first to characterize the role of this signaling mechanism in HSCs and how FOXS1 relates to the development of fibrotic events in the progression of liver disease. Further, our study established FOXS1 as a liver fibrosis biomarker.

We have previously shown an extensive hepatic kinome atlas where we analyzed the spectrum of kinase activities in cirrhotic humans and rodent models of fibrosis using our advanced PamGene kinome technology (7). We found that the two species have very similar pathways activated to motivate the phenomena (the percent of data concordance was over

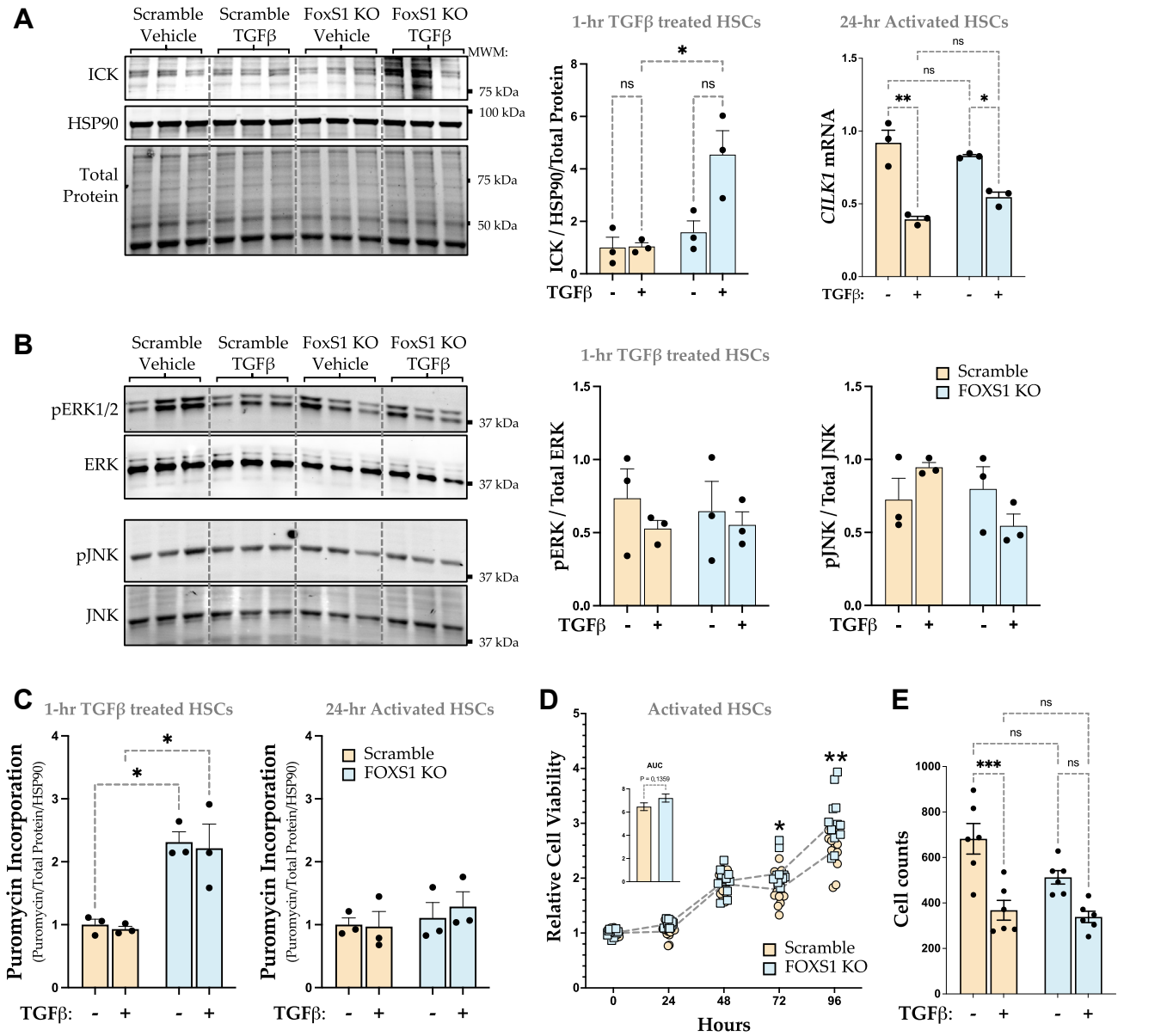

Figure 8. Validation of PamGene PamStation kinase activity profiling and functional assays. *A*, ICK protein levels were measured by immunoblotting in the FOXS1 KO and scrambled control LX2 HSCs treated with TGFβ or vehicle for 1 h. ICK mRNA levels (*CILK1* gene) were measured in 24-h TGFβ activated FOXS1 KO and scrambled control cells. *$p < 0.05$; n = 3. *B*, phospho and total ERK and JNK proteins were measured in FOXS1 KO and scrambled control LX2 cells after 1-h TGFβ treatment. *C*, protein translation assays using puromycin incorporation for the 1-h TGFβ treated and 24-h TGFβ activated FOXS1 KO and scrambled control cells. *D*, cell proliferation rates in the FOXS1 KO and scrambled control LX2 HSCs were measured in response to TGFβ treatment compared to the LX2 scramble cells over 96 h *$p < 0.05$; **$p < 0.01$; (n = 12). *E*, transwell migration assays with TGFβ treatments in the FOXS1 KO and scrambled control LX2 HSCs. ***$p < 0.001$; (n = 6). ERK, extracellular-signaling regulated kinase; FOXS1, Forkhead box S1; HSC, hepatic stellate cell; ICK, intestinal cell kinase; TGFβ, transforming growth factor beta.

80%). There was a surprising finding in this comprehensive study that the insulin receptor (*INSR*) was hyperactive in the HSCs of cirrhotic humans and mouse models of fibrosis. The *INSR* expression was increased in the FOXS1 KO and with TGFβ, it was lower in the FOXS1 KO, but not significantly. The other most active tyrosine kinase was the discoidin domain receptor 1, whose ligand is collagen, which increases during fibrosis. In this study, the loss of FOXS1 caused significantly higher *INSR* and domain receptor *1* expression and significantly reduced levels of *ACTA2* (aSMA) and *COL1A1*. These indicate that FOXS1 may be paramount in activating human HSCs to commence fibrosis.

Our results shed light on the TGFβ-FOXS1–mediated mechanisms that may be responsible for proliferation and migration. The RNA-seq data suggests a perturbed transcriptional profile associated with TGFβ-FOXS1 signaling and suggests that over 400 genes may be regulated by this signaling axis. The analysis found that FOXS1 regulates pathways that control translation. Using our PamGene PamStation technology, we found kinase drivers that may be responsible for these effects in the FOXS1 KO HSCs. One signaling factor is ICK, which has been demonstrated to be involved in the proliferation, differentiation, and control of protein translation *via* mammalian target of rapamycin and Raptor (18, 19).

Interestingly, the ICK promoter (gene name is ciliogenesis-associated kinase 1) is responsive to other forkhead transcription factors, FOXA1 and FOXA2, and possibly FOXD1 and FOXJ2 (22). The ICK promoter contains multiple consensus motifs for several FOX-family transcription factors that FOXA1 and FOXA2 have been shown to increase luciferase activity by 10- to 20-fold in HEK293T cells. In the FOXS1 KO HSCs, we found that TGFβ significantly induced ICK expression but not in the scrambled cells with intact FOXS1. These suggest that FOXS1 and FOXA2 have inverse roles in regulating liver fibrosis and its development. A study by Wang *et al.* showed that FOXA2 attenuates HSC activation and fibrosis in a murine model of CCl_4-induced liver fibrosis (23). In this same mouse model, we show that FOXS1 was significantly increased with liver fibrosis and confirmed these findings in human cirrhotic livers, an irreversible end-stage hepatic fibrosis.

Our findings here suggest the TGFβ–FOXS1 axis inhibits ICK to block differentiation and guide the HSCs to proliferate, which we demonstrated that the loss of FOXS1 increased growth rates. The activation of HSCs commences with signaling that induces proliferation, which causes retinoic acid and lipid stores to be excreted and, as they continue to grow, shed their extracellular matrix proteins, such as collagen, causing liver scarring. Our data suggest that FOXS1 is activated directly by TGFβ to induce HSC activation and differentiation, contributing to the pathogenesis of liver fibrosis. Our bioinformatic analysis suggests that FOXS1 controls other factors such as protein localization to chromosomes and Cajal bodies, peptide biosynthetic process, and ribonucleoprotein complex biogenesis. The Cajal bodies are found in the nucleus of proliferative cells and regulate the cell cycle (24). The peptide biosynthetic process and ribonucleoprotein complex biogenesis are involved in protein translation. Our results show that the loss of FOXS1 causes higher growth rates, migration, and dysregulation of genes involved in the HSC activation in liver fibrosis.

FOXS1 has been recently identified to be activated by TGFβ and might be a critical component in the process of EMT transition in HCC, and correlates with poor survival rates (11). However, we did not observe that FOXS1 is increased in patients with HCC. Others have shown that TGFβ induces FOXS1 expression (11, 25). Carson *et al.* showed that TGFβ treatment in human LX2 HSCs increased several genes as they measured by RNA-seq, and one of their top-induced genes was FOXS1 (56.49-fold) with the TGFβ treatments (25). Our study is the first to determine the role of FOXS1 in the TGFβ activation of HSCs, its signaling mechanisms, and the kinase pathways it controls. Foundational studies of forkhead transcription factors suggest that in normal tissues, FOXS1 is minimal or not expressed (26), which is thought to be due to hypermethylation of the *FKHL18* gene (11, 27). Whether targeting FOXS1 for therapeutic use is possible is unknown. However, our studies here suggest that FOXS1 impacts the development of liver fibrosis. One caveat is that once the liver scarring has occurred, it is considered irreversible, and no drugs have been shown to reverse the scarring. Further understanding the role of FOXS1 in this aspect of the disease is critical.

In conclusion, the data here demonstrate that FOXS1 has a role in hepatic fibrosis pathways through TGFβ-induced signaling mechanisms. We have also identified that FOXS1 may serve as a biomarker for liver fibrosis and HSC activation. There is little to no literature to suggest the specific role of FOXS1 in liver fibrosis, and more studies are needed to determine its function. Some published work has demonstrated that FOXS1 inhibits cell growth and proliferation in certain cancerous cell lines but exhibits the opposite effect in others (28). Our studies here provide previously unknown mechanisms and pathways controlled by FOXS1. We did not find a role for FOXS1 in liver cancer but there could be specific instances that it might be increased, such as if it were fatty liver–related mechanisms that cause the HCC compared to alcohol or other factors. This study shows that FOXS1 is a liver fibrosis biomarker, and testing other fibrotic tissues for FOXS1 levels would be of value to determine if its role is specific to liver fibrosis or all fibrotic events. The expression level of FOXS1 as a biomarker of liver fibrosis should be considered in future studies, and the function of FOXS1 in normal and diseased liver should also be further determined. FOXS1 may be an early detection biomarker of hepatic fibrosis or a treatment target for end-stage liver disease. These concepts suggest a need to study the function of FOXS1 in more detail and its mechanisms concerning liver function in health and disease.

Experimental procedures

Human subjects

The human HCC tumor and adjacent nontumor tissue samples were obtained from the Markey Cancer Center Biospecimen Procurement and Translational Pathology Shared Resource Facility at the University of Kentucky under an IRB-approved protocol (Markey Cancer Center General Specimen Banking Protocol 70872). The Human Subjects Committee of the University of Kansas Medical Center approved all studies using the human cirrhotic and their control samples, as we have previously described in (7). The demographic data for the human samples are shown in Tables S1 and S2. The human studies reported abide by the Declaration of Helsinki principles.

Animal experimentation

The CCl_4 administration to mice was approved by the Institutional Animal Care and Use Committee at the Cleveland Clinic.

Statistical analyses

The kinome array and upstream kinase identification, interaction network analysis, pathway and annotation enrichment analysis, and correlation analysis are described further in the Supplemental methods. ANOVA or Student *t* test was performed on data to detect statistical differences between

control and experimental groups. p values ≤ 0.05 were considered statistically significant.

All procedures, methods, and analyses are described in more detail in the Supporting information.

Data availability

RNA-seq data and full kinase reports are available on the GitHub repository at the following https://github.com/The-Hinds-Lab/FOXS1-Is-Increased-In-Liver-Fibrosis—Kinase-Files.

The fastq files have been deposited in SRA at the following project number PRJNA1055909.

Supporting information—This article contains supporting information.

Acknowledgments—We thank the Liver Center Tissue Bank at the University of Kansas Medical Center for providing the human liver specimens used in this study supported by NIGMS grant 5P20GM144269. The authors also thank Dr Laura E. Nagy of the Cleveland Clinic for providing the mouse samples of fibrosis for the study, which was supported by NIH grant P50AA024333, and the COCVD COBRE Pathology Core at the University of Kentucky for preparing and staining human and mouse livers used for histology in the study. The cirrhotic specimens used in this study were provided by the Biorepository of the University of Kansas Liver Center and Kansas Center for Metabolism and Obesity Research, supported by NIGMS grant 5P20GM144269. This research was supported by the University of Kentucky Office of the Vice President for Research through the Diabetes and Obesity Research Priority Area.

Author contributions—E. A. B., Z. A. K., W.-H. L., L. W., K. N. B., J. F. C., and T. D. H. J. methodology; E. A. B., Z. A. K., W.-H. L., G. J. M., S. N. P., J. F. C., G. B. A., R. N. H., M. X., M. E. C. B., M. E. S., and T. D. H. J. investigation; E. A. B. and Z. A. K. formal analysis; E. A. B. and T. D. H. J. writing-original draft; E. A. B., Z. A. K., W.-H. L., G. J. M., L. W., K. N. B., S. N. P., J. F. C., G. B. A., R. N. H., M. X., M. E. C. B., M. E. S., and T. D. H. J. writing-review and editing.

Funding and additional information—This work was not supported by grant funding. However, author salaries were supported by grants during the studies from the National Institutes of Health (NIH) R01DK121797 (T. D. H. J.), R01DA058933 (T. D. H. J.), K01DK128022 (R. N. H.) and F31HL170972 (Z. A. K.), as well as the American Heart Association (23CDA1051959) and University of Toledo Foundation (J. F. C.). NIH grants P50AA024333 and P30CA177558 supported the mouse and human HCC samples, respectively. The content is solely the responsibility of the authors and does not necessarily represent the official views of the National Institutes of Health.

Conflict of interest—The authors declare that they have no conflicts of interest with the contents of this article.

Abbreviations—The abbreviations used are: DEG, differentially expressed gene; EMT, epithelial-mesenchymal transition; ERK, extracellular-signaling regulated kinase; FOXS1, Forkhead box S1; GO, Gene Ontology; HCC, hepatocellular carcinoma; HSC, hepatic stellate cell; ICK, intestinal cell kinase; INSR, insulin receptor; NAFLD, nonalcoholic fatty liver disease; NASH, nonalcoholic steatohepatitis; PTK, protein-tyrosine kinase; SMA, smooth muscle actin; STK, serine-threonine kinase; TGFβ, transforming growth factor beta.

References

1. Creeden, J. F., Gordon, D. M., Stec, D. E., and Hinds, T. D., Jr. (2021) Bilirubin as a metabolic hormone: the physiological relevance of low levels. *Am. J. Physiol. Endocrinol. Metab.* **320**, E191–E207
2. Badmus, O. O., Hillhouse, S. A., Anderson, C. D., Hinds, T. D., and Stec, D. E. (2022) Molecular mechanisms of metabolic associated fatty liver disease (MAFLD): functional analysis of lipid metabolism pathways. *Clin. Sci. (Lond)* **136**, 1347–1366
3. Lee, W. H., Najjar, S. M., Kahn, C. R., and Hinds, T. D., Jr. (2023) Hepatic insulin receptor: new views on the mechanisms of liver disease. *Metabolism* **145**, 155607
4. Godoy-Matos, A. F., Silva Junior, W. S., and Valerio, C. M. (2020) NAFLD as a continuum: from obesity to metabolic syndrome and diabetes. *Diabetol. Metab. Syndr.* **12**, 60
5. Fernando, D. H., Forbes, J. M., Angus, P. W., and Herath, C. B. (2019) Development and progression of non-alcoholic fatty liver disease: the role of advanced Glycation end products. *Int. J. Mol. Sci.* **20**, 5037
6. Badmus, O. O., Hinds, T. D., Jr., and Stec, D. E. (2023) Mechanisms linking metabolic-associated fatty liver Disease (MAFLD) to Cardiovascular Disease. *Curr. Hypertens. Rep.* **25**, 151–162
7. Creeden, J. F., Kipp, Z. A., Xu, M., Flight, R. M., Moseley, H. N. B., Martinez, G. J., *et al.* (2022) Hepatic kinome atlas: an in-Depth identification of kinase pathways in liver fibrosis of humans and rodents. *Hepatology* **76**, 1376–1388
8. Weaver, L., Hamoud, A. R., Stec, D. E., and Hinds, T. D., Jr. (2018) Biliverdin reductase and bilirubin in hepatic disease. *Am. J. Physiol. Gastrointest. Liver Physiol.* **314**, G668–G676
9. Friedman, S. L. (2008) Mechanisms of hepatic fibrogenesis. *Gastroenterology* **134**, 1655–1669
10. Frangogiannis, N. (2020) Transforming growth factor-beta in tissue fibrosis. *J. Exp. Med.* **217**, e20190103
11. Bévant, K., Desoteux, M., Angenard, G., Pineau, R., Caruso, S., Louis, C., *et al.* (2022) TGFβ-induced FOXS1 controls epithelial–mesenchymal transition and predicts a poor prognosis in liver cancer. *Hepatol. Commun.* **6**, 1157–1171
12. Bates, E. A., Kipp, Z. A., Martinez, G. J., Badmus, O. O., Soundarapandian, M. M., Foster, D., *et al.* (2023) Suppressing hepatic UGT1A1 increases Plasma bilirubin, lowers Plasma Urobilin, Reorganizes kinase signaling pathways and lipid species and improves fatty liver disease. *Biomolecules* **13**, 252
13. Badmus, O. O., Kipp, Z. A., Bates, E. A., da Silva, A. A., Taylor, L. C., Martinez, G. J., *et al.* (2023) The loss of hepatic PPARalpha in mice causes hypertension and cardiovascular disease. *Am. J. Physiol. Regul. Integr. Comp. Physiol.* **325**, R81–R95
14. Rockey, D. C., Weymouth, N., and Shi, Z. (2013) Smooth muscle α actin (Acta2) and myofibroblast function during hepatic wound healing. *PLoS One* **8**, e77166
15. Bideyan, L., Nagari, R., and Tontonoz, P. (2021) Hepatic transcriptional responses to fasting and feeding. *Genes Dev.* **35**, 635–657
16. Rui, L. (2014) Energy metabolism in the liver. *Compr. Physiol.* **4**, 177–197
17. Hinds, T. D., Jr., Adeosun, S. O., Alamodi, A. A., and Stec, D. E. (2016) Does bilirubin prevent hepatic steatosis through activation of the PPARalpha nuclear receptor? *Med. hypotheses* **95**, 54–57
18. Fu, Z., Kim, J., Vidrich, A., Sturgill, T. W., and Cohn, S. M. (2009) Intestinal cell kinase, a MAP kinase-related kinase, regulates proliferation and G1 cell cycle progression of intestinal epithelial cells. *Am. J. Physiol. Gastrointest. Liver Physiol.* **297**, G632–G640
19. Wu, D., Chapman, J. R., Wang, L., Harris, T. E., Shabanowitz, J., Hunt, D. F., *et al.* (2012) Intestinal cell kinase (ICK) promotes activation of mTOR

complex 1 (mTORC1) through phosphorylation of Raptor Thr-908. *J. Biol. Chem.* **287**, 12510–12519
20. Sakthianandeswaren, A., Elso, C. M., Simpson, K., Curtis, J. M., Kumar, B., Speed, T. P., *et al.* (2005) The wound repair response controls outcome to cutaneous leishmaniasis. *Proc. Natl. Acad. Sci. U. S. A.* **102**, 15551–15556
21. Solhi, R., Lotfi, A. S., Lotfinia, M., Farzaneh, Z., Piryaei, A., Najimi, M., *et al.* (2022) Hepatic stellate cell activation by TGFbeta induces hedgehog signaling and endoplasmic reticulum stress simultaneously. *Toxicol. In Vitro* **80**, 105315
22. Sturgill, T. W., Stoddard, P. B., Cohn, S. M., and Mayo, M. W. (2010) The promoter for intestinal cell kinase is head-to-head with F-Box 9 and contains functional sites for TCF7L2 and FOXA factors. *Mol. Cancer* **9**, 104
23. Wang, W., Yao, L. J., Shen, W., Ding, K., Shi, P. M., Chen, F., *et al.* (2017) FOXA2 alleviates CCl(4)-induced liver fibrosis by protecting hepatocytes in mice. *Sci. Rep.* **7**, 15532
24. Jady, B. E., Richard, P., Bertrand, E., and Kiss, T. (2006) Cell cycle-dependent recruitment of telomerase RNA and Cajal bodies to human telomeres. *Mol. Biol. Cell* **17**, 944–954
25. Carson, J. P., Robinson, M. W., Ramm, G. A., and Gobert, G. N. (2021) RNA sequencing of LX-2 cells treated with TGF-beta1 identifies genes associated with hepatic stellate cell activation. *Mol. Biol. Rep.* **48**, 7677–7688
26. Cederberg, A., Betz, R., Lagercrantz, S., Larsson, C., Hulander, M., Carlsson, P., *et al.* (1997) Chromosome localization, sequence analysis, and expression pattern identify FKHL 18 as a novel human forkhead gene. *Genomics* **44**, 344–346
27. Liu, Y., Tu, M., and Wang, L. (2022) Pan-cancer analysis predicts FOXS1 as a Key target in prognosis and tumor immunotherapy. *Int. J. Gen. Med.* **15**, 2171–2185
28. Wang, S., Ran, L., Zhang, W., Leng, X., Wang, K., Liu, G., *et al.* (2019) FOXS1 is regulated by GLI1 and miR-125a-5p and promotes cell proliferation and EMT in gastric cancer. *Sci. Rep.* **9**, 5281